Electron Paramagnetic Resonance of the Aluminum Interstitial in Silicon†

KEITH L. BROWER
Sandia Laboratories, Albuquerque, New Mexico 87115
(Received 25 June 1969)

Electron-paramagnetic-resonance spectra of the Al^{++} interstitial (Si-*G*18) produced in aluminum-doped (*p*-type) silicon by room temperature or 4°K electron irradiations are presented and show that the Al^{++} is located in the tetrahedral interstitial site. The hyperfine interactions with the Al^{27} and surrounding Si^{29} atoms indicate that the wave function for the paramagnetic electron is localized mostly within ~5 Å of the Al^{++} and that within this region the surrounding lattice has T_d symmetry. From a qualitative description of this wave function in terms of a molecular orbital, an attempt has been made to assign the Si^{29} superhyperfine lines observed in the Si-*G*18 spectrum to particular lattice sites. The ground-state energy level for this paramagnetic electron is on or below the substitutional aluminum acceptor level. From energy arguments, it appears that this electron is in a localized resonant state within the valence band or in a bound state in the band gap below the bottom of the valence band.

I. INTRODUCTION

In unirradiated silicon, the electron-paramagnetic-resonance (EPR) spectra of shallow substitutional acceptor impurities, such as aluminum, are not observed unless the crystal is subjected to uniaxial stress.[1] However, following an electron irradiation of aluminum-doped silicon, Watkins[2] observed a new spectrum (Si-*G*18) which he attributed to interstitial Al^{++}. Watkins's arguments[2] concerning the identity of this defect are as follows: (1) The large isotropic Al^{27} ($I_{Al}=\frac{5}{2}$, 100% abundant) hyperfine interaction, the isotropic *g* value near that of the free electron, and a total angular momentum of $\frac{1}{2}$ as evident from the Si-*G*18 spectrum suggest an Al^{++} in the $^2S_{1/2}$ state. (2) Partially resolved Si^{29} superhyperfine interactions at nearest- and next-nearest-neighbor shells are consistent with an interstitial configuration but not the substitutional one. (3) The Al^{++} interstitials are observed to migrate at ~200°C, a temperature region generally characteristic of interstitial impurity atom diffusion, to form new centers (Si-*G*19, 20, 21).

Various configurations for interstitials in the diamond-type lattice have been proposed.[3,4] Ludwig and Woodbury[5] have found that many of the transition-group impurities occupy the tetrahedral interstitial site in a variety of charge states. Although the specific interstitial configuration for the Al^{++} was not defined by Watkins, his measurements[2] indicate that the *g* tensor and the aluminum hyperfine tensor are both isotropic, which suggest from symmetry arguments that the Al^{++} is in a site of tetrahedral symmetry.

This paper presents new experimental data and an analysis of the Si^{29} superhyperfine lines associated with the Al^{27} hyperfine lines in the Si-*G*18 spectrum. These studies establish the position of the Al_i^{++} in the lattice. They also give information on the nature of the wave function for the paramagnetic electron as well as the nature of the surrounding lattice. Both EPR and electron-nuclear double-resonance (ENDOR) data on the Si^{29} superhyperfine resonances are presented which show that the Al_i^{++} occupies the tetrahedral interstitial site in silicon. An unambiguous assignment of the various Si^{29} superhyperfine interactions associated with particular silicon neighbors is not obvious because of the lack of knowledge concerning wave functions associated with deep levels in silicon. The assignment of the various Si^{29} superhyperfine interactions is made on the basis of a molecular-orbital calculation. Also considered is the position of the ground-state energy level for this paramagnetic electron relative to the band structure of silicon.

II. EXPERIMENT

A. Experimental Techniques

The samples were aluminum-doped Lopex silicon (*p*-type, 0.721–0.792 Ω cm) which had been electron irradiated with 2 MeV electrons at either 4 or ~310°K with fluences up to 10^{17} e/cm^2. The EPR spectra were observed under the following typical conditions: $T\simeq 25$°K, $P_{\text{microwave}}\simeq 1$ μW, $Q_{\text{loaded}}\simeq 6000$ (TE_{011} cavity), $H_{\text{modulation}}\simeq 0.05$ Oe at ~100 Hz, and a sweep rate of $\lesssim 10$ Oe/min. For these conditions the absorption signal of the Si-*G*18 resonance is completely saturated and unobservable, but the dispersion signal is unsaturated and 90° out-of-phase with the magnetic field modulation. According to the criteria of Portis,[6] the Si-*G*18 spectrum under these conditions is observed in adiabatic rapid passage for which an absorptionlike resonance is expected. No resonances were observed in the unirradiated material.

The ENDOR spectra were observed while monitoring the electron spin resonance in the dispersion mode with

† Work supported by the U. S. Atomic Energy Commission.
[1] G. Feher, J. C. Hensel, and E. A. Gere, Phys. Rev. Letters **5**, 309 (1960).
[2] G. D. Watkins, in *Radiation Damage in Semiconductors*, edited by P. Baruch (Academic Press Inc., New York, 1964), p. 97.
[3] K. Weiser, Phys. Rev. **126**, 1427 (1962).
[4] J. W. Corbett, in *Radiation Effects in Semiconductors*, edited by F. L. Vook (Plenum Publications, Inc., New York, 1968), p. 3.
[5] G. W. Ludwig and H. H. Woodbury, in *Solid State Physics*, edited by F. Seitz and D. Turnbull (Academic Press Inc., New York, 1962), Vol. 13, p. 223.
[6] A. M. Portis, Technical Note No. 1, Sarah Mellon Scaife Radiation Laboratory, University of Pittsburgh, 1955 (unpublished).

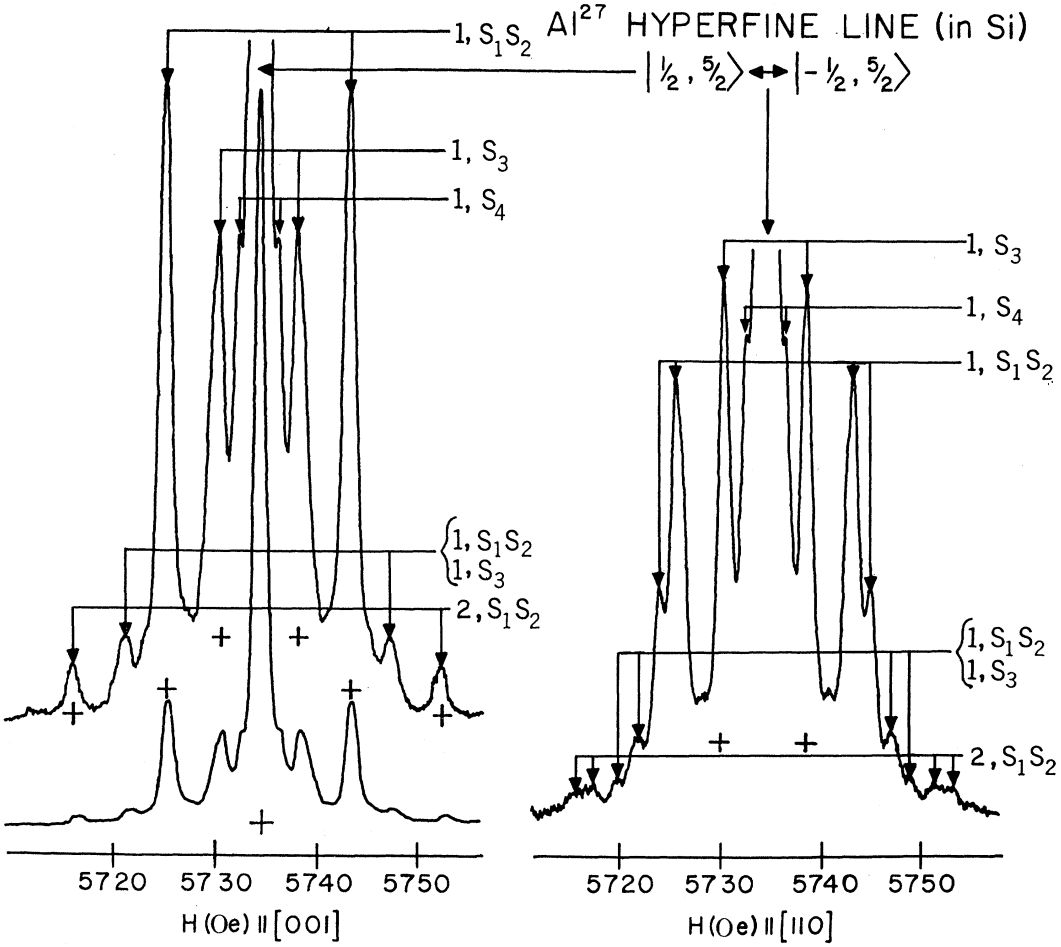

FIG. 1. EPR spectra of one of the aluminum HF lines and associated Si^{29} SHF structure for $H\|[001]$ and $H\|[110]$. These spectra were observed at 25°K and 19.486 GHz from aluminum-doped silicon following a room-temperature irradiation of 10^{17} e/cm^2. For $H\|[001]$, the upper spectrum was observed with a gain factor five times that of the lower spectrum. The spectrum for $H\|[110]$ illustrates the asymmetry in the envelopes of the S_1S_2 Si^{29} SHF lines. The heights of the resonances in Fig. 4 were measured from the respective crosses.

100 Hz magnetic field modulation at 10°K and ~ -30 dBm of incident microwave power. The rf power, which was supplied by an IFI 510 wideband amplifier driven by a HP 606B signal generator, was applied to a single loop of wire wrapped around the sample.[7]

B. Spectra

The Si-*G*18 spectrum consists of six aluminum hyperfine (HF) lines. The lowest-field aluminum HF line is shown as the central line in Fig. 1. The orientation of the magnetic field with respect to the crystal lattice was determined from the angular dependence of the $(V+V)^+$ spectrum (Si-*G*6),[8] which is also produced as a result of the electron irradiation. The $(V+V)^+$ spectrum is not shown. The structure on the sides of the aluminum HF line is due to the superhyperfine (SHF) interaction with neighboring Si^{29} atoms.[2] The various lines in Fig. 1 correspond to various configurations of neighboring Si^{29} atoms and are identified by the nomenclature K,S_m or K,S_mS_n where K corresponds to the number of Si^{29} atoms in the neighborhood of the Al_i^{++} and S_m (or S_mS_n) is the particular neighbor shell(s) in which those K Si^{29} atoms are located. (The subscript m does not imply nearest-neighbor order.) These lines have a full width at half-maximum of 1.2 Oe. Incandescent light only reduces the intensity of this spectrum. After the light has been turned off, the spectrum recovers its original intensity over a period of approximately 10 min at $\sim$25°K. No detectable changes in the EPR spectrum of the Al_i^{++} are observed due to stress up to 660 kg/cm^2 along the [110] at 25°K, although the effects of the same stress on the $(V+V)^+$ center are very pronounced.

A number of attempts under a variety of experimental conditions (temperature, microwave power, rf power, coil configuration, sweep rates, and light) have been made in order to observe the ENDOR spectra asso-

[7] G. D. Watkins and J. W. Corbett, Phys. Rev. **134**, A1359 (1964).
[8] G. D. Watkins and J. W. Corbett, Phys. Rev. **138**, A543 (1965).

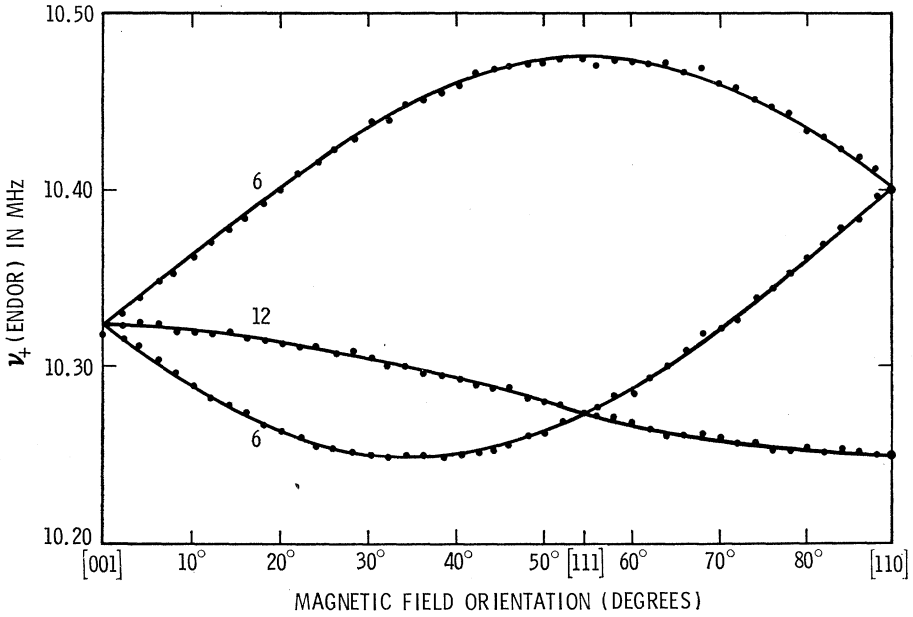

FIG. 2. ENDOR spectrum of the S_4 lines in Fig. 1. The relative intensities of these lines are as indicated. The dots correspond to the experimental data and the solid lines to the calculated ENDOR frequencies.

ciated with the Si^{29} SHF lines. The various ENDOR lines are usually quite weak, but we did succeed in obtaining the complete ENDOR spectrum associated with the 1, S_4 EPR line. This spectrum is shown in Fig. 2. Weak ENDOR lines associated with either the S_1 or S_2 resonance for $H\|[001]$ were also observed.

III. SPECTRUM ANALYSIS

A. Angular Dependence of Spectral Lines

The EPR and ENDOR spectra for the Si-*G*18 lattice defect can be described by a spin Hamiltonian of the form

$$\mathcal{H}=\beta\mathbf{H}\cdot\mathbf{g}\cdot\mathbf{S}+\mathbf{S}\cdot\mathbf{A}\cdot\mathbf{I}-\gamma\beta_n\mathbf{H}\cdot\mathbf{I}+\sum_i(\mathbf{S}\cdot\mathbf{A}_i\cdot\mathbf{I}_i-\gamma_i\beta_n\mathbf{H}\cdot\mathbf{I}_i). \quad (1)$$

Because there is no fine structure associated with the spectrum in Fig. 1, which would be present as predicted by second-order terms in the aluminum HF interaction *if* $S>\frac{1}{2}$, we conclude that the effective spin S for this center is $\frac{1}{2}$. Consequently, no terms bilinear in the spin operators S_x, S_y, and S_z are required in Eq. (1). In the absence of any neighboring impurity atoms or atoms of the host lattice having nuclear moments, the EPR spectrum of the *aluminum* HF lines can be represented by the first three terms in Eq. (1). For the special case in which **g** and **A** are isotropic, the eigenvalues for this part of the spin Hamiltonian are given exactly by the Breit-Rabi formula.[9] If the paramagnetic electron interacts with neighboring nuclei having nonzero magnetic moments, in particular Si^{29}, then the terms in the summation of Eq. (1) must be included.

[9] G. Breit and I. I. Rabi, Phys. Rev. **38**, 2082 (1931).

The eigenvalues for the full spin Hamiltonian can be determined either by diagonalizing Eq. (1) or by an appropriate perturbation calculation. In the strong-field approximation, the eigenstates are to first order $|S=\frac{1}{2},M;I=\frac{5}{2},m;I_i=\frac{1}{2},m_i\rangle$. The EPR spectra can be determined by taking the differences between eigenvalues in which $|\Delta M|=1$ and $\Delta m=\Delta m_i=0$, whereas the ENDOR spectra for the Si^{29} atoms of the host lattice can be determined by taking the differences between eigenvalues in which $\Delta M=\Delta m=0$ and $|\Delta m_i|=1$.

The most general forms for the tensors in this spin Hamiltonian depend upon the symmetries involved for the defect.[10] For example, for the Al^{++} to exist in a site of tetrahedral symmetry (T_d), the **g** and **A** tensors must be invariant under the transformations of the point group T_d which means that

$$\mathbf{g}=\mathbf{R}(T_d)^\dagger\mathbf{g}\mathbf{R}(T_d), \quad (2a)$$

$$\mathbf{A}=\mathbf{R}(T_d)^\dagger\mathbf{A}\mathbf{R}(T_d). \quad (2b)$$

Under the constraints of tetrahedral symmetry, **g** and **A** must be isotropic. However, for the Al^{++} to exist in the hexagonal interstitial site, **g** and **A** must be invariant under the transformations of the point group C_{3v} which allows these tensors to be axially symmetric about the $\langle 111\rangle$. Interstitial sites of lower symmetry would impose fewer constraints upon these tensors. Since the **g** and **A** tensors are observed to be isotropic[2] and the paramagnetic electron does interact significantly with neighboring atoms of the host lattice, as evident in Fig. 1, it is very likely that the Al^{++} is in a tetrahedral site, for which **g** and **A** are isotropic. For any other site, the symmetry does not require **g** and **A** to be isotropic.

[10] F. K. Kneubühl, Physik Kondensierten Materie 1, 410 (1963).

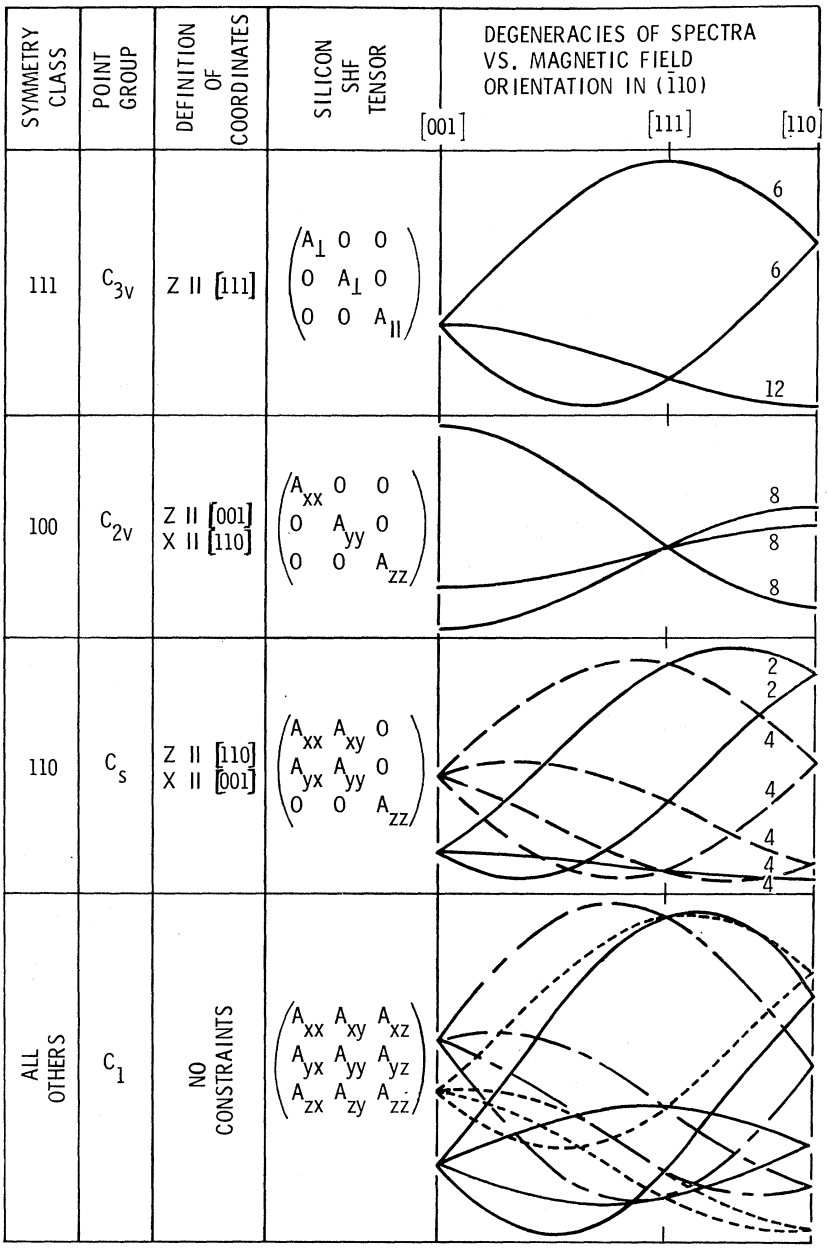

FIG. 3. Classification of the subgroups to which all the possible Al_i^{++}, Si pairs belong. The minimal constraints on the respective Si^{29} SHF tensors are tabulated. The degeneracies in the Si^{29} SHF spectra for orientations of H within the $(\bar{1}10)$ plane are illustrated assuming that $\mathbf{A}_i$ is at least symmetric. For the symmetry class which is invariant under C_1, all spectral lines are twofold degenerate.

If the Al^{++} is in a site of tetrahedral symmetry, either interstitial or substitutional, then every silicon atom of the host lattice falls into one of four symmetry classes.[10] Each class can be characterized by a subgroup of the point group T_d whose transformations on the lattice leave the orientation of a particular Al^{++}, Si pair in that class unchanged. Applying Eq. (2b), the symmetry constraints on $\mathbf{A}_i$ in Eq. (1) can be determined for the respective subgroup of each class, and these are tabulated in Fig. 3. A particular Al^{++}, Si^{29} pair can be placed in the lattice in a number of equivalent orientations; but with the application of a magnetic field, the pairs within this set are no longer all equivalent to each other. The manner in which this equivalence is broken depends upon the direction of the magnetic field. The respective symmetry class is characterized by the angular dependence of the degeneracies in the spectral lines as illustrated in Fig. 3. The relative intensity of each spectral line is indicative of the number of configurations which remain equivalent to each other in the presence of the magnetic field. The maximum number of distinct spectral lines corresponding to a particular class and set of Si^{29} neighbors is equal to the index of the respective subgroup.

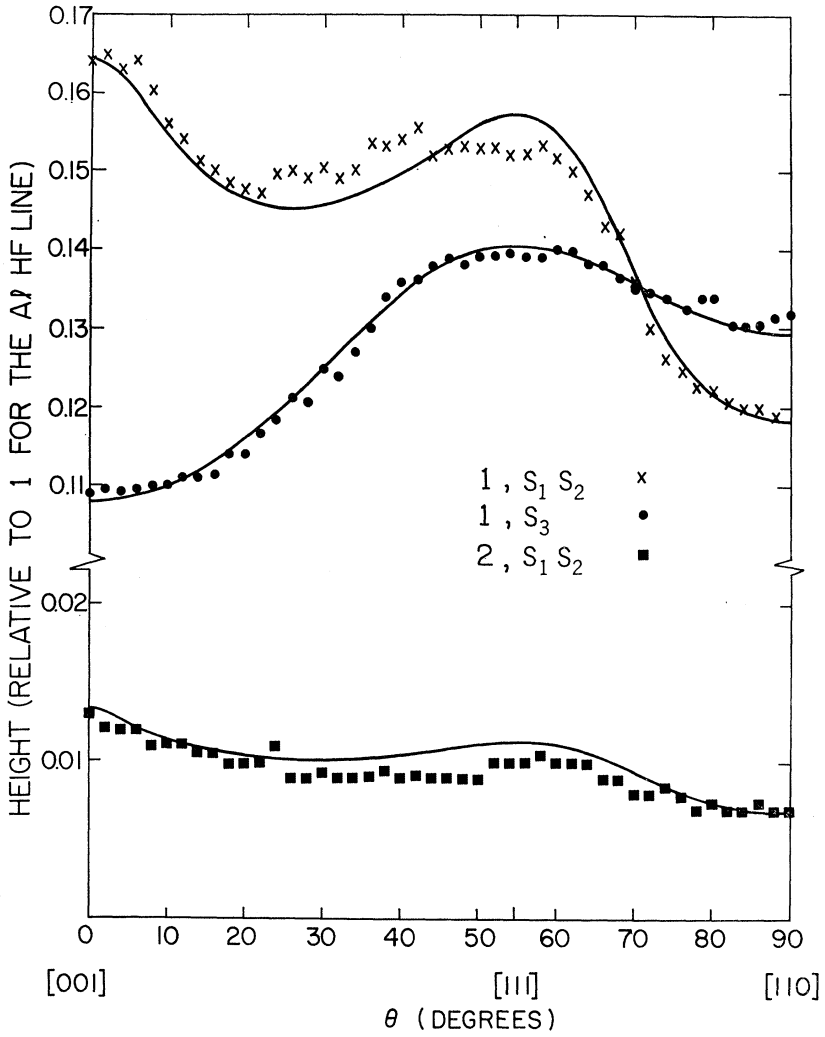

FIG. 4. Heights of the various Si^{29} SHF lines as a function of magnetic field orientation in the (1̄10) with approximately a ±2% uncertainty. The solid lines correspond to the calculated heights using the parameters listed in Table I.

As evident from Fig. 1, the Si^{29} SHF tensors corresponding to the resonances S_1, S_2, S_3, and S_4 are not sufficiently anisotropic so that the spectral lines composing these resonances are resolved to the extent that the patterns in Fig. 3 are readily recognized. Since the sum of the areas under each of the observed resonance lines belonging to a SHF line of a particular neighbor shell is constant as a function of magnetic field orientation, changes in the height and width of that observed resonance line as a function of magnetic field orientation are indicative of the anisotropy in that SHF tensor. Because these lines are narrow, ~1.2 Oe at half-height, the height of any particular resonance line is quite sensitive to small anisotropies in the respective Si^{29} SHF tensor. For any particular defect model, one can predict the angular dependence of the spectrum from Eq. (1). Assuming a certain line shape for the spectral lines in such a spectrum, one can calculate the envelope corresponding to the observed resonance line and try to fit its angularly dependent height to the observed heights by varying the elements in the corresponding SHF tensor subject to the symmetry constraints of the defect model.

B. Intensity of Si^{29} SHF Resonances

The area under a particular Si^{29} SHF resonance is proportional to the number of defects belonging to a particular configuration of Si^{29} neighbors. Suppose that there are n_k silicon atoms in the neighbor shell called S_k, corresponding to the Si^{29} SHF resonance S_k, of which m_k are Si^{29} atoms. The probability for $m_1, m_2, \ldots, m_f$ Si^{29} atoms in the neighbor shells $S_1, S_2, \ldots, S_f$ is $P_{m_1,m_2,\ldots,m_f}$ where

$$P_{m_1,m_2,\ldots,m_f}=D^M(1-D)^{N-M}\prod_{k=1}^{f}\frac{n_k!}{m_k!(n_k-m_k)!}, \tag{3a}$$

$$M=\sum_{k=1}^{f} m_k, \tag{3b}$$

TABLE I. Tabulation of the absolute values (except where signs are indicated) of the parameters in Eq. (1) for the Si-*G*18 spectrum which fit our experimental data in a least-squares analysis. The nuclear magnetic moments are measured in units of nuclear magnetons.

Parameters for the Al^{27} HF spectrum	Parameters for the Si^{29} SHF spectra in units of 10^{-4} cm^{-1}	Definition of coordinates	Symmetry class
$g=2.0019\ \pm0.0003$[a]	S_1: $A_{\parallel}=\ 21.1\ \pm0.5$	$z\|\|[111]$	111
$A=0.04402\pm0.00005$ cm^{-1} [a]	$A_{\perp}=\ 15.6\ \pm0.5$		
$\mu_n^{Al}=+3.6385$[b]	S_2: $A_{\parallel}=\ 17.0\ \pm0.5$	$z\|\|[111]$	111
	$A_{\perp}=\ 16.5\ \pm0.5$		
	S_3: $A_{xx}=\ 7.0\ \pm0.5$	$z\|\|[100]$	100
	$A_{yy}=\ 7.0\ \pm0.5$	$x\|\|[011]$	
	$A_{zz}=\ 8.6\ \pm0.5$		
	S_4: $A_{\parallel}=-3.875\pm0.01$	$z\|\|[111]$	111
	$A_{\perp}=-3.721\pm0.01$		
	$\mu_n^{Si}=-0.55477$[b]		

[a] The g value and aluminum HF parameter A have previously been measured by Watkins (Ref. 2).
[b] Varian Associates, Nuclear Magnetic Resonance Table, 4th ed., 1964 (unpublished).

and

$$N=\sum_{k=1}^{f} n_k. \tag{3c}$$

In Eq. (3a), D is equal to the fractional natural abundance of Si^{29}, i.e., $D=0.047$. Configurations of Si^{29} atoms beyond the S_f neighbor shell are accounted for in the sense that they produce the inhomogenous broadening of the resonance lines. The relative intensity of either of the two Si^{29} SHF lines labeled S_k due to a configuration of neighboring silicon atoms in which $m_j=\delta_{jk}$, $j=1, 2, \ldots, m_f$ is $n_kD(1-D)^{N-1}/(2I+1)$. The relative intensity of the observed aluminum HF line is $P_{0,0,\ldots,0}+0.5(P_{2,0,\ldots,0}+P_{0,2,\ldots,0}+\cdots+P_{0,0,\ldots,2})$. The last set of terms accounts for the contribution due to Si^{29} pairs —the probability for more complex configurations being insignificant or else unresolvable.

If the height of the observed envelope of spectral lines is to be a measure of their intensities, then the height must be measured at a magnetic field angle for which all the spectral lines belonging to a particular Si^{29} configuration coalesce. For the special cases in which $\mathbf{A}_i$ belongs to the 111 or 100 class of Si^{29} neighbors, the field positions of all the spectral lines of a particular EPR transition and SHF tensor are degenerate for $H\|[001]$ or [111], respectively, as illustrated in Fig. 3. The heights of the resonances in Fig. 1 are measured from the extrapolated tail of the aluminum HF line indicated by the positions of the crosses in Fig. 1. The observed height of the aluminum HF line is normalized to 1.

C. Analysis of Si^{29} SHF Resonances

An analysis of the angular dependence and intensity of the Si^{29} SHF resonances has allowed us to determine (1) the particular symmetry class, (2) the number of equivalent sites, and (3) the numerical values for the respective Si^{29} SHF tensors. For example, the height of the S_3 resonance is observed to be a maximum for $H\|[111]$ (see Fig. 4) which suggests its symmetry class is 100 (see Fig. 3). The intensity of the S_3 resonance corresponds to six equivalent silicon sites, which again is consistent with silicon sites in the 100 symmetry class. Subject to these constraints, the parameters in the Si^{29} SHF tensor for the S_3 resonance were determined by fitting the height of the calculated envelope to the height of the observed resonance as a function of magnetic field orientation. The calculated envelope is the sum of Gaussian line shapes 1.15 Oe wide centered at magnetic field values specified by the solutions to Eq. (1). The calculated height resulting from this least-squares-fit analysis and the observed height of the S_3 resonance are plotted in Fig. 4 as a function of magnetic field orientation. The numerical values for A_{xx}, A_{yy}, A_{zz} are tabulated in Table I.

The resonance in Fig. 1 labeled S_1S_2 has a maximum height for $H\|[001]$ and an intensity corresponding to eight silicon sites which suggest that this resonance really consists of two resonances nearly superimposed and belonging to the 111 symmetry class. This fact is most clearly revealed when one observes this spectrum with $H\|[110]$. If the two resonances S_1 and S_2 were only due to a single resonance belonging to the 111 symmetry class, the envelope of the S_1S_2 resonance would have to be symmetric about its center of gravity, which is not the case as can be seen from Fig. 1 for $H\|[110]$. Furthermore, in T_d symmetry each set of equivalent silicon neighbors belonging to the 111 symmetry class consists of only four silicon neighbors and not eight. Taking this into consideration, the hyperfine parameters, $A_{\parallel}$ and $A_{\perp}$, belonging to S_1 and S_2 were determined by fitting the height of the calculated envelope to the height of the observed resonances. The result of this analysis is shown in Fig. 4, and the numerical values for these Si^{29} SHF tensors are tabulated in Table I. As a check on this analysis, the height of the 2, S_1S_2 pair lines in Fig. 1 was calculated as a function of magnetic field orientation using the values of $A_{\parallel}$ and $A_{\perp}$ for S_1 and S_2 in Table I. The result of this calculation is represented by the solid line through the squares in Fig. 4.

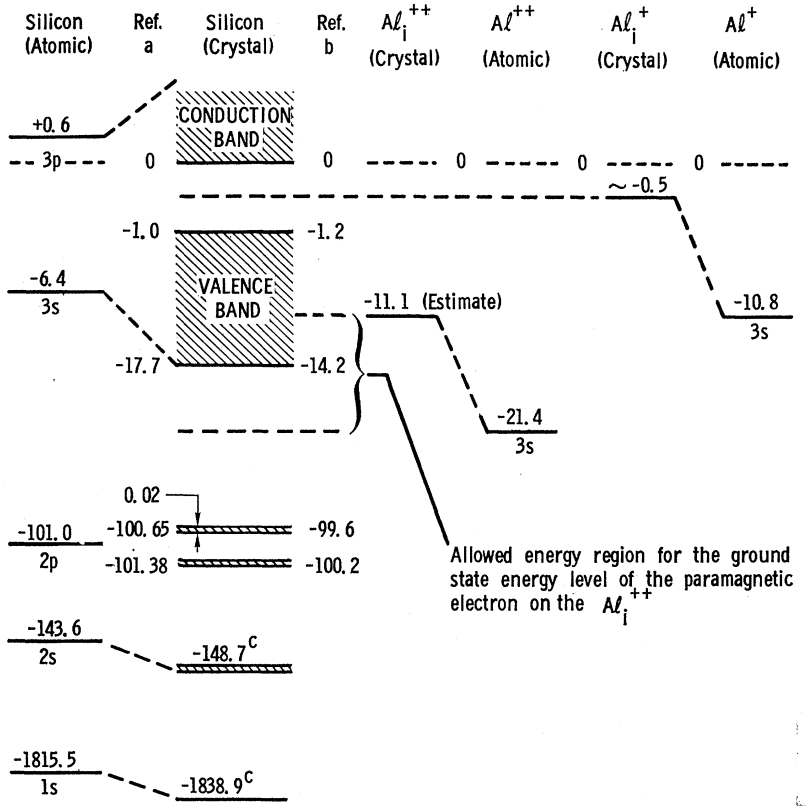

FIG. 5. Energy-level diagram. The energy-level diagram for crystalline silicon is shown as deduced from the x-ray studies of Tomboulian and Bebo (a Ref. 16) Ershov and Lukirskii (b Ref. 17) and Bearden and Burr (c Ref. 15). Also shown are the atomic levels for free Si^0, Al^+, and Al^{++} as calculated by Herman and Skillman (Refs. 18 and 19) but on an energy scale such that the $2p$ level of atomic Si^0 matches the $2p$ bands of crystalline silicon. The energy-level diagrams for Al_i^+ and Al_i^{++} *in* silicon show the expected shift of the $3s$ levels due to the interaction with the crystal.

The direct and more accurate method of determining the Si^{29} tensors is by means of ENDOR. The ENDOR spectrum associated with either S_1 or S_2 is due to Si^{29} atoms belonging to the 111 symmetry class. Other lines have also been observed but are very weak. The ENDOR spectrum corresponding to the ESR line S_4 in Fig. 1 is illustrated in Fig. 2 and clearly shows that this is an interaction with Si^{29} neighbors belonging to the 111 symmetry class. The intensity of the S_4 line in Fig. 1 is also consistent with four neighbors in this particular shell. The numerical values for this Si^{29} SHF tensor are tabulated in Table I and were determined by fitting the eigenvalues obtained by diagonalizing Eq. (1) to ENDOR frequencies associated with S_4 on three of the six aluminum HF lines ($I_z=\frac{5}{2}, \frac{1}{2}$, and $-\frac{3}{2}$).

On the basis of the analysis that has been presented, the results summarized in Table I are consistent with the assignment of the Al^{++} in a site of tetrahedral symmetry. This also means that within at least 5 Å of the Al^{++}, the surrounding lattice has T_d symmetry with respect to the Al^{++}.

IV. INTERPRETATION

A. Interstitial Versus Substitutional Site for Al^{++}

If the unpaired spin density in the region of neighboring silicon nuclei could be accurately calculated for a particular defect model, one could determine from the measured Si^{29} SHF tensors in Table I whether the Al^{++} is in the tetrahedral interstitial site or the substitutional site. Fortunately, in the case of the Al^{++}, it is possible to argue by other means that the Al^{++} is in the tetrahedral interstitial site.

The wave function which describes the paramagnetic electron in the $3s$ shell of the Al^{++} is more localized than the wave function for the shallow donors (P, As, Sb). This conclusion is based upon the observations that (1) the width of the lines in the Si-*G*18 spectrum are ~1.2 Oe as compared to~3 Oe for shallow donors (P, As, Sb),[11] (2) Ψ is more concentrated within the core of the Al^{++} than is observed in the case of these shallows donors as indicated by the proportionately larger aluminum HF interaction, and (3) the Si^{29} SHF interactions within several distinct shells of neighboring Si atoms are resolved. This last point indicates that Ψ is localized mostly within a unit cell of the diamond lattice centered on the Al^{++}.

This description of the wave function and the observation that three of the Si^{29} SHF interactions belong to the 111 symmetry class and another strong interaction belongs to the 100 symmetry class are consistent with the Al^{++} in the tetrahedral interstitial site. If the Al^{++} were in the tetrahedral substitutional site, one would expect to see a Si^{29} SHF interaction due to 12

[11] G. Feher, Phys. Rev. 114, 1219 (1959).

equivalent second-nearest-neighbor sites belonging to the 110 symmetry class. We do not observe such an interaction. Furthermore, if the Al^{++} were in the substitutional site, it is difficult to see how it could exist in this charge state since substitutional aluminum is found only in the neutral or negative charge state.

B. Position of Energy Level for Al_i^{++}

The fact that we simultaneously observe the divacancy in the positive charge state (Si-*G*6)[8] means that the Fermi level was within 0.25 eV of the valence band during the course of all our measurements. We have also observed that the production rate of the Al_i^{++} is proportional to the electron fluence at least in the range $5\times10^{14}\leq\Phi\leq10^{17}$ e/cm^2. For fluences as low as 5×10^{14}, it is believed that the Fermi level at 25°K is between the top of the valence band and the substitutional aluminum acceptor level[12] which is 0.06 eV above the valence band.[13] Consequently, the ground-state energy level for this paramagnetic electron is on or below the substitutional aluminum acceptor level.

According to Schechter,[14] the radius of Ψ for the substitutional group-III shallow acceptors is between 7 and 18 Å. From our measurements, it appears as though the wave function for the paramagnetic electron on the Al_i^{++} is more localized than Schechter's wave function for holes associated with group-III shallow acceptors. One might question whether or not the ground-state energy level for the paramagnetic electron on the Al_i^{++} is between the top of the valence band and the aluminum acceptor level.

In Fig. 5, the energy-level diagram for crystalline silicon as deduced from x-ray studies[15–17] is shown. Also shown are the one-electron ground-state energy levels for *free* Si^0, Al^{++}, and Al^+ as determined by Herman and Skillman.[18,19] In Fig. 5, the energy scale for all of the atomic levels is adjusted such that the $2p$ level for atomic silicon matches the $2p$ level for crystalline silicon. If the Al^{++} and Al^+ were embedded in the silicon crystal, one would expect the valence electrons for these centers to be more loosely bound due to dielectric effects than they are in the atomic state. According to Watkins,[2] the ground-state energy for the Al^+ is in the band gap of silicon. The difference between this energy for the $3s$ level of Al^+ in crystalline silicon and the energy for the $3s$ level in atomic Al^+ is approximately the perturbation energy (10 eV) due to the interaction of the Al^+ with the crystal. For deeper levels ($2p$, $2s$, $1s$) the perturbation energy would be smaller since the interaction of these states with the crystal is weaker by virtue of the more localized character of the core states. In the case of the Al_i^{++}, the corresponding energy difference for the $3s$ level would not be expected to exceed 10 eV. If the $3s$ level for atomic Al^{++} in Fig. 5 is raised by as much as 10 eV, it still is $\sim$10 eV below the top of the valence band.

On the basis of this argument, the energy region in which the ground-state energy level of the paramagnetic electron on the Al_i^{++} might be expected to lie is indicated in Fig. 5. The energy region overlapping the valence band has not been excluded as a possible position for the impurity level since it is conceivable that a localized resonant state could exist within the valence band.

C. Assignment of Si^{29} SHF Resonances to Neighboring Lattice Sites

In order to assign different silicon neighbor shells in the same symmetry class with particular Si^{29} SHF resonances, the wave function for the spin density, Ψ, needs to be known. The isotropic part of the hyperfine interaction, a, where

$$a_{\text{theor}}=(8\pi/3)g\beta(\mu_n/I)\beta_n|\Psi|^2 \tag{4a}$$

and

$$a_{\text{expt}}=\tfrac{1}{3}\,\text{Tr}(\mathbf{A}), \tag{4b}$$

is a measure of the spin polarization at the respective nucleus. The anisotropic part of the hyperfine interaction, b_α, where

$$b_{\alpha_{\text{theor}}}=(g\beta\mu_n\beta_n/I)\langle\Psi|\,(3x_\alpha^2-r^2)/r^5|\Psi\rangle \qquad (\alpha=1,\,2,\,3 \text{ principal axis}) \tag{5a}$$

and

$$b_{\alpha_{\text{expt}}}=\mathbf{n}_\alpha\cdot\mathbf{A}\cdot\mathbf{n}_\alpha-a_{\text{expt}} \quad (\mathbf{A}\text{ diagonal}), \tag{5b}$$

is due to the asymmetry in the spin polarization immediately surrounding the respective nucleus.

A proper quantum-mechanical treatment of this center which would give Ψ is beyond the scope of this paper. However, an attempt has been made to represent the spin polarization by a wave function for the paramagnetic electron associated with the Al_i^{++}. This phenomenological wave function

$$\Psi(\mathbf{x})=N\{\psi_{3s}+\sum_{kl}[\alpha_{kl}\Phi_{kl}{}^A+\beta_{kl}\Phi_{kl}{}^B]\} \tag{6}$$

is represented by a $3s$-like orbital within the immediate vicinity of the Al_i^{++} plus an admixture of all the bonds, bonding and antibonding, which are tetrahedrally coordinated to the silicon atoms shown in Fig. 6. This wave function is constructed so that it transforms as Γ_1 under the operations of the point group T_d. The

[12] H. J. Stein (private communication).
[13] M. Neuberger, EPIC AD 601 788, 1964 (unpublished).
[14] D. Schechter, J. Phys. Chem. Solids **23**, 237 (1962).
[15] J. A. Bearden and A. F. Burr, Rev. Mod. Phys. **39**, 125 (1967).
[16] D. H. Tomboulian and D. E. Bebo, Phys. Rev. **104**, 590 (1956).
[17] O. A. Ershov and A. P. Lukirskii, Fiz. Tverd. Tela **8**, 2137 (1966) [English transl.: Soviet Phys.—Solid State **8**, 1699 (1967)].
[18] F. Herman and S. Skillman, *Atomic Structure Calculations* (Prentice-Hall, Inc., Englewood Cliffs, N. J., 1963).
[19] The computer program for doing atomic structure calculations was obtained indirectly from Herman and Skillman through D. E. Harrison, Jr., who had adapted this program to the CDC 3600 at Sandia.

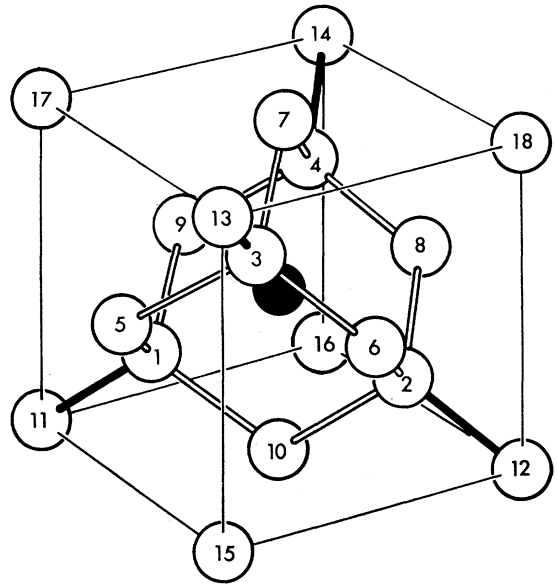

FIG. 6. Aluminum ion indicated by the shaded ball is in the tetrahedral interstitial site. Sites 1–4 correspond to 1 nn; sites 5–10 to 2 nn; sites 11–14 to 4*a*, nn; and sites 15–18 to 4*b*, nn.

admixture of bonding and antibonding orbitals corresponds qualitatively to the admixture of states from the valence and conduction bands, respectively. The effects of charge polarization within the neighboring bonds, spin core polarization, and displacement of silicon atoms from their normal lattice sites[20] have not been taken into consideration.

An attempt was made to associate the resonances S_1, S_2, and S_4, which all belong to the 111 symmetry class with specific lattice sites using the expression for $\Psi(\mathbf{x})$ in Eq. (6). One is faced with two problems. First, is the expression for $\Psi(\mathbf{x})$ in Eq. (6) an adequate description of the spin polarization, and second, if it is, how does one calculate from first principles the α_{kl} and β_{kl}? Assuming that $\Psi(\mathbf{x})$ is an adequate description of the spin polarization, $|\Psi(\mathbf{x})|^2$ was evaluated at various lattice sites assuming that the absolute magnitudes of α_{kl} and β_{kl} are inversely related to the distance between the Al^{++} and the respective bonds, which is roughly the case if α_{kl} and β_{kl} are determined by orthogonalizing $\Psi(\mathbf{x})$ to $\Phi_{kl}{}^A$ and $\Phi_{kl}{}^B$. It is observed that $|\Psi(\mathbf{x})|^2$ is smaller on 4*b*, nn atoms (sites 15–18 in Fig. 6) than on either 1 nn, 2 nn, or 4*a*, nn sites. At the same time, it is possible for $|\Psi(\mathbf{n})|^2$ on 4*a*, nn silicon atoms to be of the same magnitude as $|\Psi(\mathbf{x})|^2$ on 1 nn silicon atoms. These two neighbor shells are directly bonded to each other.

The resonances S_1, S_2, and S_4 are due to a Si^{29} SHF interaction with only one Si^{29} atom in the vicinity of the Al_i^{++}. We surmise that the S_1 resonance is due to a Si^{29} atom in the 1 nn shell (1–4) and that the S_2 resonance is due to a Si^{29} atom in the 4*a*, nn shell (11–14), or vice versa. The distinction can not be made using Eq. (6) in Eqs. (4a) and (5a). The S_4 resonance is believed to be due to a Si^{29} atom in the 4*b*, nn shell (15–18).

The S_3 resonance is due to a single Si^{29} atom in the vicinity of the Al_i^{++} and in the 2 nn shell (sites 5–10 in Fig. 6). This conclusion is based on the observation that the S_3 resonance belongs to the 100 symmetry class and the belief that Ψ is localized mostly within the unit cell shown in Fig. 6.

V. SUMMARY

The fact that the **g** tensor and the aluminum HF tensor **A** in the spin Hamiltonian of Eq. (1) are both isotropic indicates that the Al^{++} is very likely in a site of tetrahedral symmetry. More specifically, the symmetry of the Si^{29} SHF interaction tensors, $\mathbf{A}_i$, and the intensity of the respective Si^{29} SHF lines are only compatible with the Al^{++} in the tetrahedral interstitial site. Consequently, within at least 5 Å of this Al_i^{++}, the surrounding lattice has T_d symmetry.

Our EPR measurements indicate that the ground-state energy level for the paramagnetic electron associated with the Al_i^{++} is below the substitutional aluminum acceptor level. From the localized character of this wave function and energy arguments, it appears that the ground-state energy level for the paramagnetic electron of the Al_i^{++} is $\sim$10 eV below the top of the valence band but above the 3*s* atomic level of free Al^{++} on an energy scale matching that for crystalline silicon.

Since the tail of the 3*s* orbital for *free* Al^{++} would overlap with neighboring silicon atoms of the host lattice if it were placed in the tetrahedral interstitial site, one might expect the wave function to be more accurately represented by a molecular orbital of the form in Eq. (6). Although this description of the wave function is not adequate for accurately determining the isotropic and anisotropic hyperfine interactions for a particular defect model, it does give insight into the interference effects which appear to exist in the actual wave function as evident from the anisotropies in the spin density at neighboring Si^{29} nuclei. The width of the lines in the Si-*G*18 spectrum and the hyperfine interactions indicate that the wave function for this paramagnetic electron is localized mostly within the unit cell shown in Fig. 6. From the molecularlike character of this wave function, we surmize that resonances S_1, S_2, and S_4 arise from a Si^{29} atom in 1 nn (sites 1–4 in Fig. 6), 4*a*, nn (11–14) (or 4*a*, nn, 1 nn), and 4*b*, nn (15–18)

[20] Radial displacements of neighboring silicon atoms with respect to the Al_i^{++} are compatible with the observation that the Al^{++} is in a site of tetrahedral symmetry. Assuming that the electric dipole moments induced in neighboring silicon atoms are proportional to the electric field and that small displacements of the silicon atoms from their normal lattice sites are proportional to the electrostatic force exerted upon the polarized silicon atoms, the small displacement of a silicon atom from its normal lattice site would in a first approximation be inversely proportional to the fifth power of the distance between the Al_i^{++} and the respective silicon atom.

sites, respectively. The S_3 resonance is due to a Si^{29} atom in the 2 nn shell.

ACKNOWLEDGMENTS

Discussions with D. K. Brice, H. J. Stein, A. C. Switendick, F. L. Vook, and G. D. Watkins on various aspects of this work have been particularly helpful. G. D. Watkins suggested the possibility that the Si^{29} SHF interactions (S_1 and S_2) might be explained on the basis of an oscillatory character in the wave function without invoking a large lattice distortion. The competent assistance of N. D. Wing in many of the measurements is very much appreciated.

PHYSICAL REVIEW B VOLUME 1, NUMBER 5 1 MARCH 1970

Spin-Lattice Relaxation in a Γ_8 Quartet: Er^{3+} in MgO

M. Borg, R. Buisson, and C. Jacolin
Laboratoire de Spectrométrie Physique, Faculté des Sciences de Grenoble, France*
(Received 19 May 1969)

The orbit-lattice Hamiltonian for rare-earth ions is obtained using a new approach in which it is not necessary to calculate the normal modes of the cluster consisting of the central ion and its first neighbors. The determination of the parameters describing the first-order orbit-lattice coupling is greatly simplified, whatever the environment. The problem of relaxation of a Γ_8 ground quartet is then studied. The equations of evolution of the populations are solved for one-phonon and two-phonon processes, and the relaxation times are calculated. It is shown that, under certain initial conditions, two relaxation times are sufficient. The angular variation for the one-phonon process is established. The calculations are greatly simplified by noting relations between matrix elements which were obtained from local symmetry and time-reversal considerations. The experimental results on $MgO:Er^{3+}$ verify the existence of two relaxation times and confirm their predicted angular variation. The discrepancy (a factor of 4) between experimental and theoretical values is discussed.

I. INTRODUCTION

THERE are some cases in which the splitting of the ground term of a rare-earth ion by the cubic-crystalline field results in a quartet as the ground state. This quartet, which can appear only in Kramers ions, is associated with the Γ_8 representation of the O_h group. Bleaney[1] and Ayant *et al.*[2] have developed the theory of these quartets. EPR has shown their existence and, among them, the $MgO:Er^{3+}$ system has been studied in great detail.[3,4] It is of interest to pursue this work by studying the spin-phonon coupling in this system.

Much attention has been devoted to the theoretical and experimental study of spin-phonon coupling in rare-earth ions.[5–11] But the special case of Γ_8 has never been considered theoretically,[12] and we know of only one experiment in which an attempt was made to measure the relaxation time, that of Bierig *et al.*[13] on $CaF_2:Dy^{3+}$. In their case, the relaxation time was too short to be observed. Dobrov[14] tried to measure the spin-phonon coupling by acoustic resonance, but his results were not fully explained. We shall see that the behavior of $MgO:Er^{3+}$ is, on the contrary, well understood.

In Sec. II of this paper, we deduce the orbit-lattice Hamiltonian expression, using a new approach, and we show that, for direct and Orbach processes, it is not necessary to consider only the cluster consisting of the ion and its first neighbors. We arrive at the same formal result as Orbach but with a more general meaning for the parameters describing the coupling. In addition, the calculation of these parameters for each particular case is greatly simplified, as we indicate in the Appendix. In Secs. III and IV, we give the outline of the calculation of the relaxation times due to the direct process for a Γ_8 quartet, with application to the case of $MgO:Er^{3+}$. The full use of symmetry considerations enables us to find relations between matrix elements and to show that

* Laboratoire associé au C.N.R.S.

[1] B. Bleaney, Proc. Phys. Soc. (London) **B73**, 937 (1959).

[2] Y. Ayant, E. Belorizky, and J. Rosset, J. Phys. Radium **23**, 201 (1962).

[3] D. Descamps and Y. Merle d'Aubigné, Phys. Letters **8**, 5 (1964).

[4] E. Belorizky, Y. Ayant, D. Descamps, and Y. Merle d'Aubigné, J. Phys. **27**, 313 (1966).

[5] R. Orbach, Proc. Roy. Soc. (London) **A264**, 458 (1961).

[6] P. L. Scott and C. D. Jeffries, Phys. Rev. **127**, 32 (1962).

[7] Cha-Yuan-Huang, Phys. Rev. **139**, A241 (1965).

[8] R. C. Mikkelson and H. J. Stapleton, Phys. Rev. **140**, A1968 (1965).

[9] E. S. Sabisky and C. H. Anderson (unpublished).

[10] A. A. Manenkov and R. Orbach [*Spin Lattice Relaxation in Ionic Solids* (Harper & Row Publishers, Inc., New York, 1966)] give a review of the general problem of the relaxation until 1966.

[11] R. Orbach and M. Blume, Phys. Rev. Letters **8**, 478 (1962).

[12] In Ref. 11, R. Orbach and M. Blume have cited the case of a Γ_8 ground state only to give an example where the T^{-5} temperature dependence of spin-lattice relaxation time could hold.

[13] R. W. Bierig, M. J. Weber, and S. I. Warshaw, Phys. Rev. **134**, A1504 (1964).

[14] W. I. Dobrov, Phys. Rev. **146**, 268 (1966).